論文 / 著書情報
Article / Book Information

Title	Study on a Practical Robotic Follower to Support Home Oxygen Therapy Patients -Development and Control of a Mobile Platform-
Author	Atsushi Tani, Gen Endo, Edwardo F. Fukushima, Shigeo Hirose, Masatsugu Iribe, Toshio Takubo
Journal/Book name	, , , pp. 2423-2429
Issue date	2011, 9
DOI	http://dx.doi.org/10.1109/IROS.2011.6094633
URL	http://www.ieee.org/index.html
Copyright	(c)2011 IEEE. Personal use of this material is permitted. Permission from IEEE must be obtained for all other users, including reprinting/republishing this material for advertising or promotional purposes, creating new collective works for resale or redistribution to servers or lists, or reuse of any copyrighted components of this work in other works.
Note	このファイルは著者（最終）版です。 This file is author (final) version.

Study on a Practical Robotic Follower to Support Home Oxygen Therapy Patients -Development and Control of a Mobile Platform-

Atsushi Tani, Gen Endo, Edwardo F. Fukushima, Shigeo Hirose, Masatsugu Iribe and Toshio Takubo

***Abstract*— Home oxygen therapy (HOT) is a medical treatment for patients suffering from severe lung diseases. Although walking outdoors is recommended for patients to maintain physical strength, patients always have to carry a portable oxygen supplier which is not sufficiently light weight for this purpose. Our ultimate goal is to develop a mobile robot to carry an oxygen tank and follow a patient in an urban outdoor environment. We have proposed a mobile robot with a tether interface to detect the relative position of the foregoing patient. In this paper, we improve mobile platform mechanisms and active wheels to maximize the step height which can be negotiated, and to allocate sufficient space in the main body to carry an actual oxygen tank. The following control algorithm is also improved and its effectiveness is demonstrated in an outdoor experiment.**

I. INTRODUCTION

Home oxygen therapy (HOT) is a physician-prescribed treatment for patients suffering from severe lung diseases such as Chronic Obstructive Pulmonary Disease (COPD). Breathing supplemental oxygen through the nose via cannula increases the amount of oxygen in the blood, usually reducing shortness of breath and other symptoms, allowing more independent life and increasing survival. By introducing an oxygen concentrator, HOT can maintain the quality of life of the patients because they can live in their home. There are many pieces of home medical equipment and services providers and HOT is fully covered by health insurance in Japan. It is reported that over 150,000 people get HOT treatment in Japan [1].

An appropriate exercise, such as a walk, is recommended for COPD patients to keep physical strength. Figure1 shows a commonly used portable equipment for going out. However the total weight of the equipment is not lightweight: they are over $4kg$ including the carrier cart. Carrying a heavy cart may stress the lungs and become a psychological burden. Consequently, there are many patients who do not go out frequently.

A. Tani, G. Endo, E.F. Fukushima and S. Hirose are with the Dept. of Mechanical and Aerospace Engineering, Graduate School of Science and Engineering, Tokyo Institute of Technology, 2-12-1-I1-60 Ookayama, Meguro-ku, Tokyo 152-8552, Japan {gendo, fukusima, hirose}@mes.titech.ac.jp

M. Iribe is with the Faculty of Engineering, Osaka Electro-Communication University,18-8 Haccho, Neyagawa-shi, Osaka 572-8530, Japan iribe@isc.osakac.ac.jp

T. Takubo is with the First Department of Medicine, Tokyo Women's Medical University ,8-1 Kawada-cho, Shinjuku-ku, Tokyo, 162-8666, Japan ttakubo@chi.twmu.ac.jp

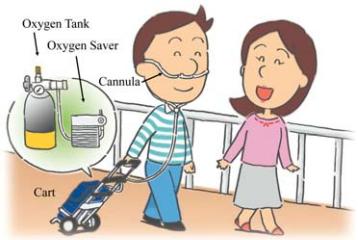

Courtesy of TEIJIN PHARMA LIMITED

Fig. 1. Portable oxygen supplier

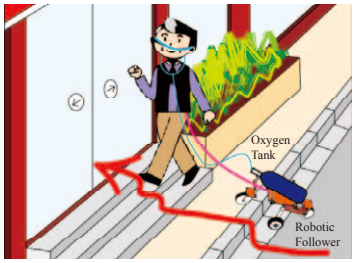

Fig. 2. Basic concept of the robotic follower carrying an oxygen tank

In this study, our ultimate goal is to develop a mobile robot to carry an oxygen tank and follow a foregoing person in an outdoor environment (Fig. 2). For a more concrete use case, we assume that "the patient goes out shopping to the nearest grocery (convenience) store". Because the main purpose of going out (except for hospital visits) is shopping in daily life. Moreover, we emphasize low cost production as much as possible, because most of the HOT patients are pensioners [2].

The robotic follower, named by [3], which is a mobile robot following a foregoing person, is not a novel idea because many previous works can be found in the literature such as [4]-[7]. However these previous works used multiple expensive wireless sensors and its application was limited to an indoor environment.

Therefore in our previous work, we proposed to utilize a tether to detect the relative position of the foregoing person to be robust and cost-effective, and developed a new mobile platform capable of negotiating a step 50mm in height, which is usually employed as a curb ramp to separate a sidewalk from the street [8].

In this paper, we improve the mobile platform mechanisms and active wheels to maximize the step height which can be negotiated, and to allocate sufficient space in the main body to carry an actual oxygen tank. The following control algorithm is also improved to accurately track the leader's trajectory.

II. Mobile Robot Platform

A. Basic Design

A mobile platform with two active wheels is one of the simplest and most cost-effective configurations. The two drive wheels are located in the middle of the robot and two passive support casters are installed in the front/back end of the body of the robot. Differential velocity control of each wheel permits steering and pivot turning. Although it is a very simple configuration, the locomotion ability on rough terrain is limited when the passive casters are rigidly fixed to the body of the robot. Thus, we focus on a chassis mechanism used in planetary exploration rovers, because the rover is required to achieve high locomotion ability. In this study, we adopt the chassis mechanism of "Hien-II", which has a rhomboid shaped wheel configuration and two bogie mechanisms connected by a differential mechanism in order to distribute body weight evenly on the wheels (Fig. 3)[9][10].

Figure 4(a) shows the linkage system of Hien II. Hien II has four active wheels and the front and middle left wheels are suspended by a bogie mechanism (red) while the rear and middle right wheels are suspended by a second bogie mechanism (light blue). Since these two bogie mechanisms are connected by a differential mechanism, such as two pulleys with a cross-multiply timing belt, when the front and rear wheels move upward, both middle wheels move downward [9][10].

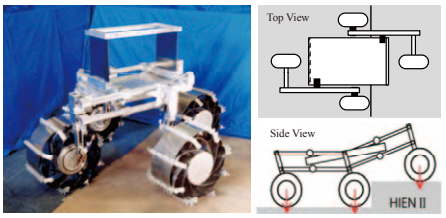

Fig. 3. Prototype model of the mars exploration rover "Hien II"

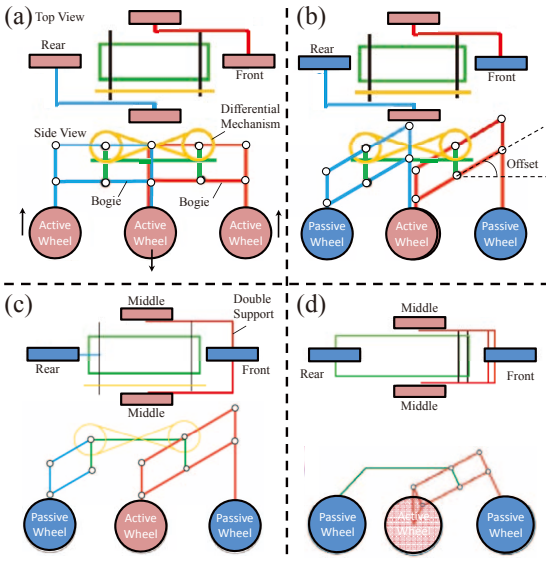

Fig. 4. Modification of the bogie link system: (a) Hien II with four active wheels, (b) introducing initial offset to the bogie links, (c) double support beam structure for the bogie links, (d) fixing the rear wheel steering axis to the body (final design)

In our application, we decided to use only two active wheels for the middle wheels, while the front/rear wheels are ordinary passive casters for mechanical simplicity. If the bogie link is completely parallel to the body, the front wheel cannot negotiate a high step because the front wheel cannot generate traction force and the bogie link fall into a singular position. To avoid this situation, we introduced an initial angular offset for the bogie links as shown in Fig. 4(b) [8]. Although this offset was effective to decrease the required traction torque of the middle wheels for climbing up a step, this mechanism did not have sufficient structural rigidity due to the cantilever structures supporting the front/rear wheels.

To solve the problem, we investigated a double support beam structure for attaching the front wheel as shown in Fig. 4(c). This configuration successfully achieved almost the same performance compared with Fig. 4(b) in the dynamics simulator, which will be explained later.

Next let us discuss the linkage for the rear passive caster. In Fig. 4(c), the rear linkage system and the differential mechanism are introduced to keep the same height as the front wheel. However focusing on the relative height of the front/rear wheels relative to the middle wheels, Fig. 4(c) can be simplified to Fig. 4(d). Although the location of the center of gravity (CG) between Fig. 4(c) and (d) during step climbing motion is slightly different due to the inclination of the main body, this effect can be handled by optimizing link parameters for the frontal bogie mechanism. (This kind of simplification is also applied in [11].) Therefore we selected the Fig. 4(d) configuration because of simplicity.

B. Static Analysis

We analyzed static balancing to derive the required traction force F generated by the middle wheels depending on the bogie link geometrical parameters. We investigated the front wheel negotiation and middle wheel negotiation, postulated as a 2-dimensional problem. We assume the radius of the wheels are identical and the middle wheel is located in the middle of wheel base W.

Figure 5 shows the link model and its parameters. L_i is the

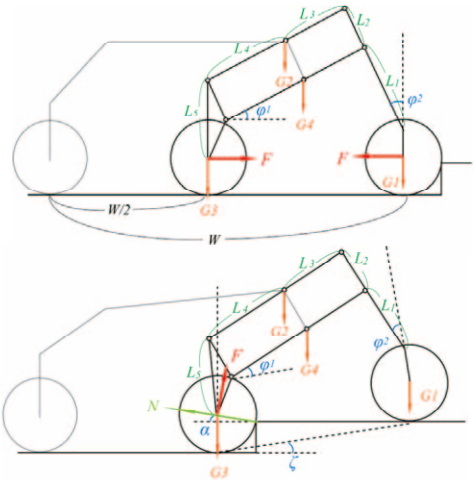

Fig. 5. Static force analysis: front wheel negotiating (top), middle wheel negotiating (bottom)

length of the link and G_j is the gravitational force. $\phi_{1,2}$ are the initial angular offsets, and α and ζ are geometrically determined angles depending on the wheel radius, wheel base and step height. In the case of front wheel negotiation, we assume the reaction force from the step is completely horizontal because of the most difficult case.

We derive the equation of equilibrium about each link and obtain the following conditions for negotiating the step.

$$F > \frac{G_1 + \frac{L_4}{L_3+L_4}(G_2+G_4)}{\tan\phi_1} \quad (1)$$

$$F > G_3\cos\alpha + (G_2+G_4)\frac{L_3}{L_3+L_4}\frac{\cos(\phi_1+\zeta)}{\cos(\phi_1+\alpha+\zeta)} \quad (2)$$

Equation (1) is for the front wheel while (2) is for the middle wheel. Equation (1) indicates that larger values for L_3 and ϕ_1 permit a smaller traction force F for front wheel negotiation. On the contrary, (2) shows the smaller L_3 and ϕ_1 provide the smaller F for the middle wheel negotiation. Thus these conditions suggest a trade-off problem for the bogie link design shown in Fig. 6.

C. Optimization of the Link Parameters using a Dynamics Simulator

In this section, we numerically derive the optimum link parameter L_3/L_4 and ϕ_1 using the dynamics simulator "Open Dynamics Engine (ODE)" [12]. The evaluation criteria are 1) equalization of the required traction force F during total step climbing, 2) maximization of acceptable step height (which should be more than 80% of the wheel radius). Figure 7 shows the geometrical relationships and mass distributions for ODE, where M is a total weight of the mobile robot and r is the radius of the wheel. These geometrical relations and mass properties are estimated based on the previous prototyping work and 3DCAD modeling. The weight of the body includes the weight of an oxygen tank and its accessories.

We measure the maximum required traction force where the step height is $0.5r$, friction coefficient between the wheel and the ground is 0.7 and velocity of the robot is 0.8 m/s achieved by velocity feedback control of the middle wheels.

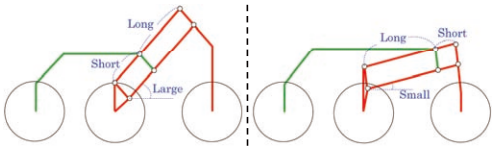

Fig. 6. Results of the static force analysis: suitable for front wheel negotiation (left), for rear wheel negotiation (right)

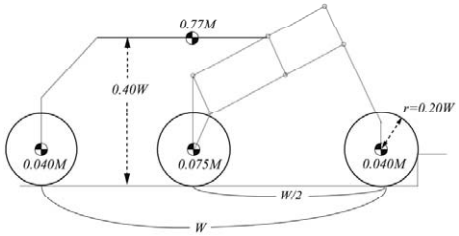

Fig. 7. Simulation model for the dynamics simulator

We vary L_3/L_4 from 0.2 to 1.6 while ϕ_1 is varied from 10 to 50 degree with 10 degree intervals. Figure 8(left) shows the simulated model in ODE and Fig. 8(right) shows the result of ϕ_1=40 deg where the traction force is normalized with respect to the total weight of the robot.

As we expected, increasing L_3/L_4 decreases required traction force for the front wheel negotiation while it needs the larger force for the middle wheel. We searched for optimum parameters which maximize the allowable step height under the condition that the required maximum force deviations between each wheel are less than 20%. Finally we obtain $L_3/L_4 = 0.8$ and $\phi_1 = 40deg$, which achieves a step height negotiation of $0.9r$. The hardware implementation of the optimized bogie link mechanism is shown in Fig. 9. The expected maximum step height is $90mm$ because its wheel base is $500mm$.

D. Low-Profile In-Wheel Motor

This mobile platform should have sufficient space to carry an oxygen tank. Moreover the total width of the robot should be as compact as possible. Figure 10 (left) shows a typical arrangement of actuators to drive the middle wheels. It is difficult to achieve sufficient range of motion of the bogie links due to the interferance between the actuator and the main body. Thus we propose a low-profile in-wheel motor as shown in Fig. 10 (right) to maximuze the luggage space while keeping the width of the robot narrow.

Figure 11 shows the basic structure of the proposed in-wheel motor. The actuator and blue and light blue parts

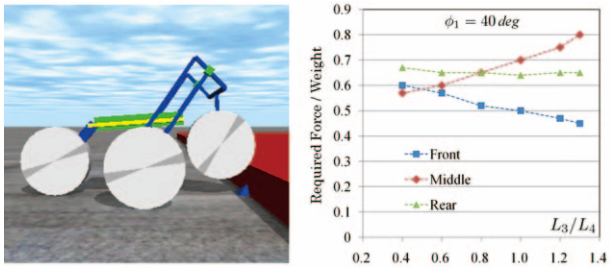

Fig. 8. An example of ODE simulation (left) and required force (right)

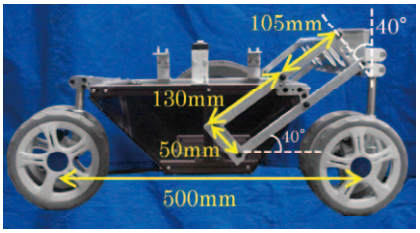

Fig. 9. Hardware implementation with the optimized link parameters (the middle wheel is not attached)

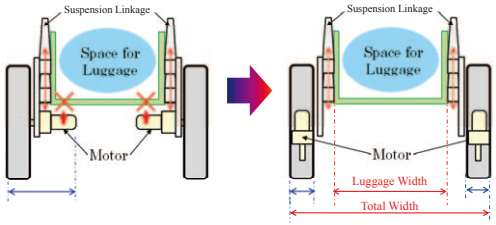

Fig. 10. Problem of the conventional actuator arrangement (left) and proposed arrangement (right)

are fixed, and thus external power lines can be connected to the actuator through the blue wheel shaft pipe. The red ring part and light red wheel are also fixed. (Note that the green part in the cross-section view is not shown in the front view.) The light red part is attached to the blue shaft via a ball bearing in order to rotate around the axis of the wheel. There is a single stage speed reducer consisting of the yellow part and the red ring part. This single stage reduction mechanism can typically be composed of bevel gears.

The proposed in-wheel motor has high space efficiency and is easily made water and dust proof. It will be cost-effctive and light weight if we can manufacture the red ring part and light red part as one part by injection molding process. Moreover we can easily increase the total output power by radially arranging the additional actuators (Fig. 11 (b)).

For prototyping, we used a ladder chain and a sprocket for the single stage speed reducer. The ladder chain is circularly glued to a grooved ring part (Fig. 12). Strictly speaking, this mechanism is not suitable for durability because the chain and the sprocket tooth generate slippage due to the difference of the tangential velocity. However this slippage can be negligible when the diameter of the wheel is large, and thus it is sufficient for our prototyping. We confirm that this mechanism can transmit sufficient torque and its efficiency is roughly estimated as 75% from preliminary experiments.

E. Tether Mechanism

We use a tether to detect the relative position between foregoing person and the mobile robot. Of course we can utilize the oxygen tube as a measurement device in the future, we use a wire for initial verification of the system because of the ease of implementation. A constant force spring (Sunco Spring: CONSTON NWS-0.25-1), which generates a constant tension of 2.45N regardless of the length of the tether, is introduced for the tether winding mechanism. The tension is assumed not to be a physical load for the patient during walking because it is sufficiently small. The length and the direction of the tether are measured by potentiometers (Fig. 13). This sensing device is significantly cost-effective and robust compared with wireless sensing devices such as a laser range finder and stereo vision camera.

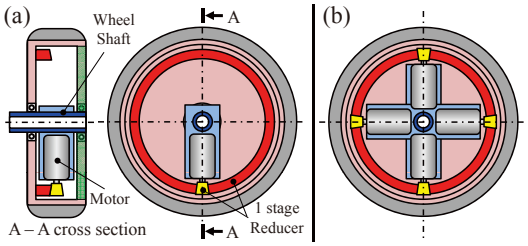

Fig. 11. Proposed low-profile in-wheel motor

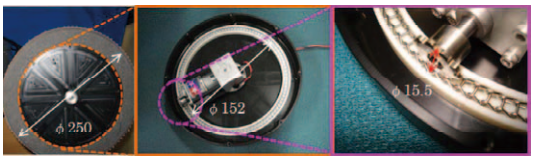

Fig. 12. Developed low-profile in-wheel motor

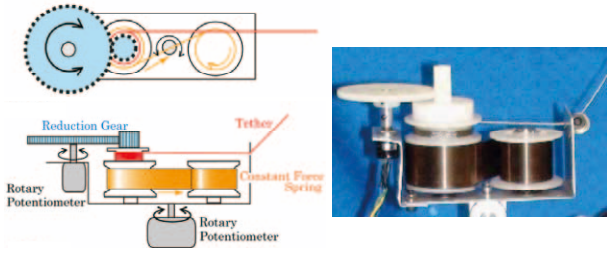

Fig. 13. Tether mechanism to measure the tether length and the direction

F. System Integration of the Mobile Platform

Figure 14 shows the integrated mobile platform. In Section II.B and C, we assume that all wheel diameters are identical to investigate the basic characteristics of the linkage system. However for the hardware implementation, we chose a smaller diameter for the front/rear wheel to maximize the luggage space. This modification does not greatly affect the performance of the maximum step height because the only traction force is provided by the middle wheels, and these passive casters are suspended by the link mechanism to help their step negotiation. The main body has sufficient space to carry an oxygen tank and its accessories.

The angular velocity of the wheels are controlled by a micro processor board (HiBot Corp: TITech SH2 Tiny Controller) via a motor driver circuit (TITech Robot Driver Ver.2) using velocity control mode. The micro processor also measures tether information to calculate the target velocity of each wheel. Table 1 shows the specification of the mobile platform.

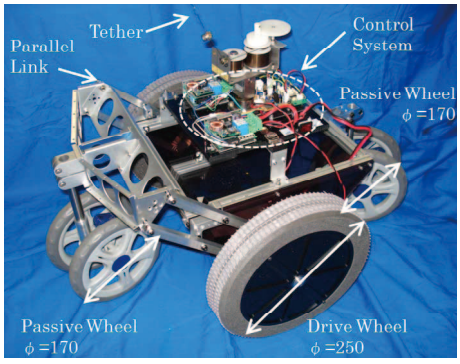

Fig. 14. Overview of the prototype

Table.1 Specification of the prototype

Dimension [W x D x H]	460 x 670 x 420 [mm]
Weight	8.8 [kg] (with tank & batteries)
Wheel diameter	170 [mm], 250[mm]
Maximum velocity	1.0 [m/s]
Battery	LEAD-ACID : 12V-2.0Ah x 2 (NP2-12, GS Yuasa)
Actuator	20[W] x 2 : Tamiya 380K20
Reduction Ratio	204
Direction angle sensor	Potentiometer
Winding angle sensor	
CPU	SH7047F CLK/44.2MHz (Hitachi)
Motor Driver	TITech Robot Driver Ver.2

III. Following Control by Hyper-Tether

In our previous work, the authors have proposed a general concept "Hyper-Tether" which covers a transmission of mechanical/electrical energy, a transmission of communication signal, a function of an automatic generation of steering commands for the leader-following and so on. Especially for the automatic generation of the steering commands, we have investigated the leader following method by measuring the direction and the length of the tether [13]. The advantages of this method for the position measurement are high reliability and cost efficiency. Our proposed algorithms to follow the leader are briefly explained and we modify it to minimize the deviation of the length of the tether in the following section.

A. Pseudo-Joystick Steering Control

The most direct implementation of a following controller is to regard the direction and the length of the tether as a steering command. The translational velocity of the follower V_r and its angular velocity Ω_r are expressed as follows.

$$V_r = -K_p(l_m - l_d)\cos\phi, \tag{3}$$

$$\Omega_r = -\frac{2V_r}{w_r}\sin\phi, \tag{4}$$

$$\phi = \theta \tag{5}$$

where l_m, l_d are the measured and desired length of the tether respectively. K_p is the velocity gain and w_r is the width of the robot. The follower moves in the direction pulled by the tether because the target moving direction ϕ equals the direction of the tether θ relative to the robot body. Finally angular velocity commands to each wheel, ω_L, ω_R, are obtained as follows,

$$\mathbf{V} = \mathbf{A}^{-1}\mathbf{q}, \tag{6}$$

where $\mathbf{V} = [\omega_L \ \omega_R]^T$, $\mathbf{q} = [V_r \ \Omega_r]$ and $\mathbf{A}$ transforms the wheel angular velocity whose wheel radius is r, to the body velocity as follows.

$$\mathbf{A} = \begin{bmatrix} r/2 & r/2 \\ -2r/w_r & 2r/w_r \end{bmatrix} \tag{7}$$

B. Follow-the-leader Control

More accurate tracking of the leader position relative to the following robot can be accomplished by monitoring the history of the tether tip. If the mobile robot can track it's own position/orientation relative to an inertial reference frame, say $\sum_g$, the tether tip's trajectory history can also be known relative to the same $\sum_g$. Here we define trajectories of the tether tip $\mathbf{T}(s_t)$ and the following robot $\mathbf{P}(s_r)$ where s_t, s_r are parameters for each trajectory, respectively. The target moving direction ϕ is derived through the following steps.

Step 1: Estimation of the follower position by dead reckoning.

i) Estimation of the translational/angular velocity at time t.

$$\mathbf{q} = \mathbf{AV} \tag{8}$$

ii) Derivation of the direction of the follower Γ relative to an inertial reference frame $\sum_g$.

$$\Gamma(t+\Delta t) = \Gamma(t) + \Omega_r(t)\Delta t \tag{9}$$

iii) Derivation of the travelling distance of the follower Δs_r.

$$\Delta s_r = V_r \Delta t \tag{10}$$

iv) Update the position of the follower $\mathbf{P}(s_r)$.

$$\mathbf{P}(s_r + \Delta s_r) = \mathbf{P}(s_r) + \mathbf{E}^{k\Theta}\begin{bmatrix}\Delta s_r \\ 0\end{bmatrix} \tag{11}$$

where $\Theta = \Gamma + \theta$ is the direction of the tether in $\sum_g$ and

$$\mathbf{E}^{k\Theta} = \begin{bmatrix}\cos\Theta & -\sin\Theta \\ \sin\Theta & \cos\Theta\end{bmatrix}. \tag{12}$$

Step 2: Derivation of the tether tip's position $\mathbf{T}(s_t + \Delta s_t)$.

$$\mathbf{T}(s_t + \Delta s_t) = \mathbf{P}(s_r + \Delta s_r) + \mathbf{E}^{k\Theta}\begin{bmatrix}l_m \\ 0\end{bmatrix} \tag{13}$$

Step 3: Derivation of the travelling distance of the tether tip.

$$\Delta s_t = ||\mathbf{T}(s_t + \Delta s_t) - \mathbf{T}(s_t)|| \tag{14}$$

Step 4: Derivation of the target moving direction ϕ.

Search a point s_{tmin} on the tether tip's trajectory $\mathbf{T}(s_t)$ which satisfies the minimum distance ρ between the follower position $\mathbf{P}(s_r + \Delta s_r)$ and $\mathbf{T}(s_t)$. Then we add a certain distance δ to s_{tmin} along to $\mathbf{T}(s_t)$ and generate the target moving direction ϕ in order to asymptotically converge $\mathbf{P}(s_r)$ to $\mathbf{T}(s_t)$ as follows.

$$\phi = \Phi - \Gamma, \tag{15}$$

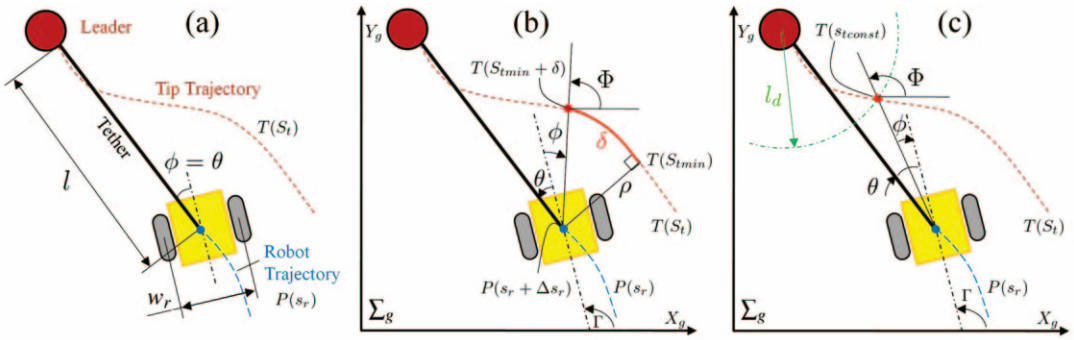

Fig. 15. Algorithm for the leader following: (a)pseudo-joystick control, (b)follow-the-leader algorithm, (c)modified follow-the-leader algorithm.

where Φ and Γ is the target moving direction and the forward direction of the follower in $\sum_g$. Finally we obtain the desired wheel velocities by using Eqn.(3),(4),(6).

This control method could successfully track the leader's trajectory with high accuracy compared with pseudo-joystick control verified by the experiment using two crawler robots [14].

C. Modified Follow-the-leader Control

The previous follow-the-leader control was proposed to improve the trajectory tracking accuracy and the distance between the leader and the follower did not have first priority although it is implicitly maintained by Eqn.(3). However, in this application, keeping the desired distance is very important because a patient and an oxygen tank is also connected by an oxygen tube whose length is limited. Additionally, the following behaviour of the previous approach tends to be unstable when the leader rapidly changes its velocity because δ in Step 4 is a no time-dependent open parameter and should be manually tuned depending on the relative velocity.

To solve these problems, we modify the target moving direction ϕ in order to explicitly keep a constant distance. Instead of $\mathbf{T}(s_{tmin}+\delta)$, we propose to use $\mathbf{T}(s_{tconst})$ which is a crossing point between $\mathbf{T}(s_t)$ and a circle with desired tether distance l_d whose center is the current leader position shown in Fig. 15(c). Moreover we introduce the following control laws instead of Eqn.(3)(4).

$$V_r = -K_p(l_m - l_d)(1 - K_a|\phi|), \quad (16)$$

$$\Omega_r = -K_b\,\phi, \quad (17)$$

where K_a and K_b are control gains. In Eqn.(3), V_r is only adjusted by $\cos\phi$ and there is no other parameter to adjust the magnitude of influence of the angular difference. Equation (16) decreases the translational velocity V_r proportional to the angular difference ϕ and its effect can be modulated by K_a. As for Ω_r, Eqn.(3) depends on V_r and the orientation of the robot cannot be controlled when $V_r = 0$. In our application, the orientation control of the robot should be always active to prevent the oxygen tube over-wound.

We evaluate the modified follow-the-leader control by using ODE. The leader walks along the black-dashed line in Fig. 16 at a constant velocity of $0.5m/s$, where l_d is set to $0.8m/s$. The result indicates that the follow-the-leader control has the best trajectory tracking accuracy and the modified algorithm has slightly lower performance. However the deviation of the tether during following shows that the modified algorithm has much smaller length change shown in Fig. 17, which is suitable for our application. Moreover we tested various walking patterns by manually controlling the leader's walking path and velocity using ODE. We verified that the modified algorithm was more stable than the previous follow-the-leader algorithm.

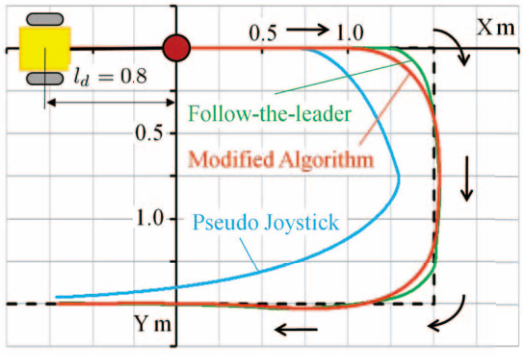

Fig. 16. Trajectory following simulation using three different algorithms: (a)pseudo-joystick control, (b)follow-the-leader control, (c)modified follow-the-leader control.

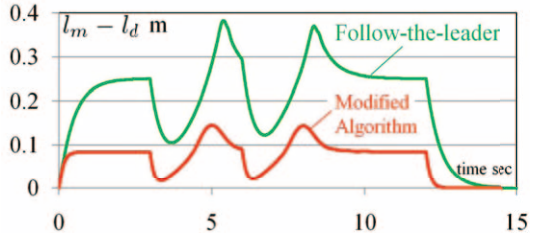

Fig. 17. Time course of the tether length deviation

IV. Experiment

A. Step Climbing Experiment

We carried out step climbing experiments to measure the maximum height of the step when the moving velocity is $0.8m/s$. We varied the step height at $5mm$ interval and confirmed the maximum height of $80mm$ (Fig. 18) , which is $10mm$ lower than ODE simulation result. However this performance is acceptable because the height of commonly used curb without a slope in Japan is $90mm$ whose edge radius is $15mm$. Figure 19 shows the curb climbing in an outdoor environment, successfully negotiating the curb.

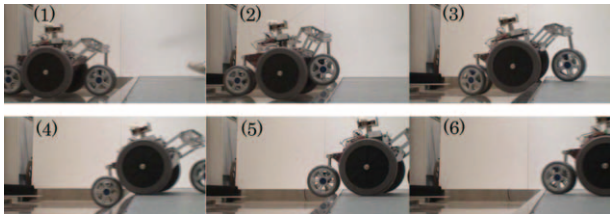

Fig. 18. Step climbing experiment: height of the step 80mm

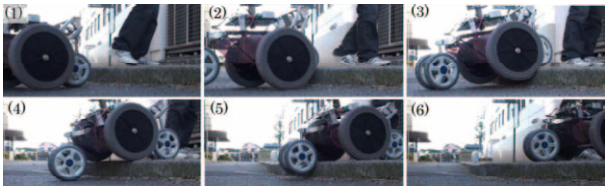

Fig. 19. Step climbing experiment: height of the curb 90mm

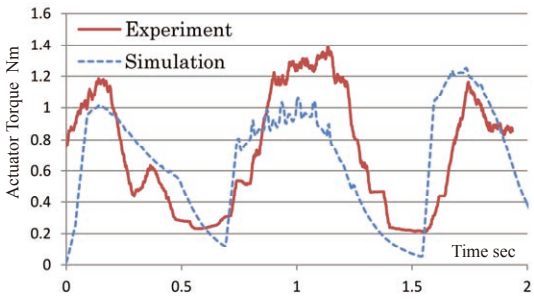

Fig. 20. Driving torque comparison between simulation and experiment negotiating 60mm height step

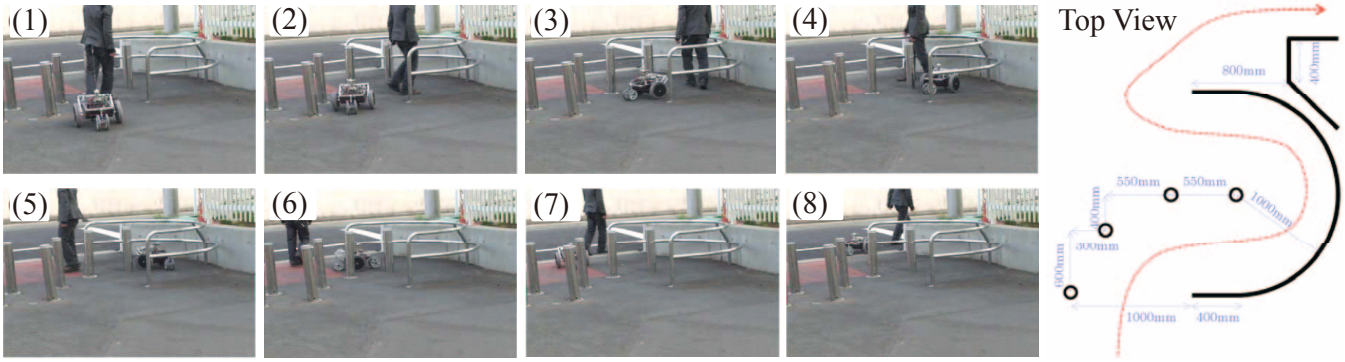

Fig. 21. An experiment passing through bollards in outdoor environment at 2.0sec interval capture (left), top view of the path (right)

The ratios of the maximum step height per wheel radius are 0.94 and 0.64 for the front/rear passive wheel and the middle drive wheel respectively. Compared with the conventional mobile robot platform whose ratio is about 0.3 [15], this result suggests that optimized bogie link mechanism is effective at increasing the step climbing ability.

Figure 20 shows the required torque of the middle drive wheel to negotiate a step height of 60mm. The experimental torque is derived by measuring the actuator current and multiplying by both torque constant of 2.75mNm/A and reduction ratio of 204. The simulation model of the platform is modified to fit the hardware implementation. The experimental torque has a similar tendency to the simulated torque and the maximum torque peaks are close. This result indicates the bogie mechanism successfully distributes the required torque of the middle wheel when each wheel climbs up the step.

B. Following Experiment in an Outdoor Environment

We demonstrated a following experiment passing through bollards in an outdoor experiment (Fig. 21(left)). The leader's path and positions of the bollards are shown in Fig. 21(right). The extremity of the tether was attached to the waist of the leader, thus the leader can freely use both hands. The mobile robot successfully followed the leader's path passing through the 1.0m width passway including a sharp turn of 0.5m radius.

Finally we carried out a following experiment assuming the actual use case. The goal is to go shopping to the nearest convenience store in our campus which is 300m away from our office on the fifth floor of the building. There is an elevator, an automatic door, a slope for a wheel chair, maintenance hatches, grating covers, a step of 50mm height and so on. The following robot successfully navigated in the above-mentioned environment and arrived at the final destination.

V. Conclusion

In this paper, we investigated a mobile platform mechanisms and active wheels to maximize the negotiable step height, and to allocate sufficient space in the main body to carry an actual oxygen tank. The following control algorithm using a tether is also improved and demonstrates its effectiveness in an outdoor following experiment.

So far we have focused on increasing the hardware performance of the following robot. However the usability of this robotic solution should be definitively evaluated by HOT patients. The specification would be modified based on the feedback from them, for example size, weight, battery capacity and so on. Additional safety sensors and fail-safe design are also very important for the practical use. We plan to carry out usability tests with HOT patients. We do hope to contribute to bettering the HOT patients' quality of life.

References

[1] K. Kida, Home Oxygen Therapy in Japan: Clinical application and considerations for practical implementation, Japan Medical Association Journal, Vol.54, No.2, pp.99-104, 2011.
[2] The Japanese Respiratory Society, *The White Paper of Home Breathing Care*, Bunkodo, 2005 (in Japanese).
[3] K. Tokuda, K. Osuka, S. Yano and T.Ono, Concept and Development of General Rescue Robot CUL, Int. Conf. on Intelligent Robots and Systems, pp.1902-1907, 1999.
[4] http://robot.watch.impress.co.jp/cda/news/2008/02/28/923.html
[5] http://inventorspot.com/articles/roboporter_robot_baggage_carts_1_10769
[6] T. Yoshimi et al., Development of a Person Following Robot with Vision Based Target Detection, Int. Conf. on Intelligent Robots and Systems, pp.5286-5291, 2006.
[7] http://robot.watch.impress.co.jp/cda/news/2007/12/10/789.html
[8] G. Endo et al., Study on a Practical Robotic Follower to Support Daily Life -Development of a Mobile Robot with "Hyper-Tether" for Home Oxygen Therapy Patients-, International Symposium on System Integration (SI International), P01, 2009.
[9] S. Hirose N. Ootsukasa T. Shirasu, H. Kuwahara and K. Yoneda, Fundamental Considerations for the Design of a Planetary Rover, Int. Conf. on Robotics and Automation, pp.1939-1944, 1995.
[10] S. Hirose, Y. Furuhashi, N. Ootsukasa, Development of 4-Wheeled Planetary Exploration Rover "Hien II", The 14th Annual Conf. of the RSJ, pp.251-252, 1996 (in Japanese).
[11] R. Siegwart, P. Lamon, T. Estier, M. Lauria and R. Piguet, Innovative design for wheeled locomotion in rough terrain, Robotics and Autonomous Systems, vol.40, pp.151-162, 2002.
[12] "Open Dynamics Engine" http://www.ode.org/
[13] E. F. Fukushima N. Kitamura and S. Hirose, A New Flexible Component for Field Robotic System, Int. Conf. on Robotics and Automation, pp.2583-2588, 2000.
[14] T. Kamagawa, E. F. Fukushima and S. Hirose, Research On Hyper-Tether No.4 Cooperative Steering Control for Multiple Robots Connected in Series, JSME Robomec, 2P1-56-083, 1999 (in Japanese).
[15] "Mobile Robotics Inc." http://www.mobilerobots.com/Mobile_Robots.aspx